Femtosecond Study of the Effects of Ions and Hydrophobes on the Dynamics of Water

Sietse T. van der Post, Klaas-Jan Tielrooij, Johannes

Hunger, Ellen H.G. Backus, and Huib J. Bakker[*]

FOM Institute AMOLF, Science Park 104, Amsterdam, The Netherlands

(Dated: June 6, 2012)

Abstract

We study the effects of ions and hydrophobic molecular groups on the orientational dynamics of water using THz dielectric relaxation (THz-DR) and polarization-resolved femtosecond infrared (fs-IR) pump-probe spectroscopy. We measure the dynamics of water in solutions of NaI, NaCl, CsCl, guanidinium chloride (GndCl) and tetramethyl guanidinium chloride (TMGndCl) of different concentrations. With THz-DR we observe that strongly hydrated cations align the static dipoles of their surrounding water molecules. With fs-IR we find that the OD groups that form hydrogen bonds to halide anions reorient with two distinct time constants of 2 ± 0.3 ps and 9 ± 1 ps. The fast process is assigned to a wobbling motion of the OD group that keeps the hydrogen bond with the anion intact. The amplitude of this wobbling motion depends on the nature of both the anion and the counter cation. The replacement of four of the six hydrogen atoms of the weakly hydrated cation guanidinium by hydrophobic methyl groups leads to an exceptionally strong slowing down of the water dynamics. Hydrophobic groups thus appear to have a much stronger effect on the dynamics of water than ions. These findings give new insights in the mechanism of protein denaturation by GndCl and TMGndCl.

---

[*]Electronic address: bakker@amolf.nl

I. INTRODUCTION

The conformation of macromolecules in aqueous media is crucial for their functioning in bi-
ological systems. Many studies have been devoted to the understanding of how these structures
are formed and how this formation can be influenced with co-solutes like salts and sugars. These
studies go back to the pioneering work of Franz Hofmeister [1]. In his 1888 paper Hofmeister dis-
cussed the influence of different salts on the precipitation of proteins, a process called salting out.
Currently, the well known Hofmeister series comprises two series of cations and anions, ordered
by their ability to salt out proteins. This property has been interpreted in terms of structure-making
and structure-breaking concepts [2], i.e. a presumed ion-induced strengthening or weakening of
the hydrogen-bond network of water over long distances. Although these concepts offer an expla-
nation of the observed (de)naturation effects according to the Hofmeister series, experimentally no
evidence was found of the supposed long range structuring influence of ions on water [3–6]. Most
ions influence the structure and dynamics of only their first solvation shell [7] and only in the (rare)
case of very strongly hydrated ions, water molecules were found to be affected over a somewhat
larger distance [8]. The exact nature of ion hydration and its relation to the (de)stabilization of the
conformation of macromolecules thus remain not well understood.

Guanidinium (see inset figure 1) is on the far end of the Hofmeister series and its chloride
salt (GndCl) is among the strongest denaturants known, causing almost all proteins to unfold
completely at a concentration of 6 mol/l [9]. There is an ongoing debate about the underlying
microscopic principles of its working mechanism. Some argue that denaturants work indirectly by
affecting the properties of water [10–12]. Dielectric relaxation spectroscopy and neutron diffrac-
tion studies on the water structure around the guanidinium ion suggest that the ion lacks a signif-
icant hydration shell [13, 14]. From these results it was concluded that the denaturation process
likely involves a direct interaction with proteins, as has been proposed for urea [14, 15]. However,
molecular dynamics (MD) simulations show surprising differences between urea and guanidinium
chloride [10, 11, 16]: it was found that urea binds to peptide groups but guanidinium does not [11].
In line with this finding, it was shown in other studies that the interaction between guanidinium
and water might be crucial in understanding its denaturing properties [12]. Finally, it should be
noted that both microscopic mechanisms for denaturation are not mutually exclusive and might in
fact both be active [17].

The substitution of the hydrogen atoms of urea by methyl groups yields the osmolyte tetra-

methyl urea (TMU). Compared to urea, TMU is an even more effective denaturant [18] and shows a profound (hydrophobic) effect on the water dynamics of its solvation shell [19]. It is therefore not surprising that previous work indicated that denaturation induced by TMU may have another microscopic origin than urea [18]. Given the fundamental differences in the nature of guanidinium chloride and urea it is interesting to study the effects of the substitution of the hydrogen atoms of the guanidinium ion by methyl groups on the molecular properties of water and the denaturation of proteins.

Over the past ten years THz dielectric relaxation (THz-DR) and polarization-resolved femtosecond infrared pump-probe (fs-IR) spectroscopy have been established as powerful tools to study water dynamics [20, 21]. Recently it was shown that these techniques can provide complementary information, as they probe different axes of the water molecule [8]. In this paper we use THz-DR and fs-IR to study the effects of electrostatic and hydrophobic interactions on the dynamics of water. We compare solutions of the strong denaturing salt guanidinium chloride and tetramethyl guanidinium chloride. To bring this into the perspective of denaturation, we compare the effectiveness of guanidinium chloride, tetramethylguanidinium chloride, urea and TMU in the denaturation of the model protein Photoactive Yellow Protein.

II.   EXPERIMENT

A.   THz Dielectric Relaxation

In THz dielectric relaxation spectroscopy the dynamics of the static dipoles of water are probed by characterizing a THz pulse after transmission through the sample. Generally, an applied electric field tends to align the permanent dipoles of the water molecules against the thermal fluctuations. The proportionality of the resulting induced macroscopic polarization and the applied field is given by the frequency-dependent dielectric function. At frequencies lower than the characteristic timescale at which reorientation processes of water molecules take place, the dipoles can follow the electric field oscillations and the built-up polarization is only limited by the thermal fluctuations of the dipole orientations. At high frequencies, the dipoles fail to follow the oscillations of the applied electric field. The transition from the low-frequency to the high-frequency domain is marked by a strong response in the imaginary dielectric function due to a phase lag in the reorienting dipoles relative to the externally applied oscillating electric field.

For pure water the maximum of the out-of-phase response is found at 20 GHz, corresponding to a timescale τ_{bulk} of ≈ 8 ps [22]. This time constant is often referred to as the Debye relaxation time and has been assigned to the timescale of the spontaneous restructuring of the hydrogen-bond network. A contribution with a much lower amplitude has been found at higher frequencies ($\sim$ 0.9 THz, $\tau_{\text{fast}} \approx 350$ fs), and has been assigned either to quick jumps of undercoordinated water [23, 24], interaction-induced components in the water relaxation mechanism [25, 26] or a small angular rotation preceding a large angle jump [27]. The low-frequency dielectric function $\hat{\epsilon}(\nu)$ of water is thus modeled as a sum of two Debye modes with different time constants τ_n,

$$\hat{\epsilon}_{H_2O}(\nu) = \frac{S_{bulk}}{1 + 2\pi i\nu\tau_{\text{bulk}}} + \frac{S_{fast}}{1 + 2\pi i\nu\tau_{\text{fast}}} + \epsilon_{\infty}, \qquad (1)$$

where ϵ_{∞} is the permittivity at infinite frequency. The fraction of water molecules that reorient with time constant τ_n is proportional to the amplitude S_n. For pure water $S_{bulk} \approx 70$ and $S_{fast} \approx 2$.

In the case of salt solutions the conductivity of the sample will contribute to the dielectric response, which can be incorporated by extending equation (1) according to,

$$\hat{\epsilon}(\nu) = \hat{\epsilon}_{H_2O}(\nu) + \frac{\sigma}{2\pi i\epsilon_0\nu}, \qquad (2)$$

where the conductivities σ are taken from the literature [13, 28–31]. The addition of ions leads to a decrease of $\hat{\epsilon}(\nu)$ (depolarization), as a result of three contributions. First, in a constant volume there is a decreased number of water molecules that contribute to the signal because of dilution when a solute is added. Second, the water molecules that bind to the ions cannot reorient in the applied electric field and contribute no longer to $\hat{\epsilon}(\nu)$. Finally there is the effect of kinetic depolarization that results from the movement of charges in an electric field. The procedures to take the dilution effects and kinetic depolarization into account are described in Ref. [32].

The far-infrared THz pulse is generated by optical rectification in a ZnTe crystal pumped by a part of the output of a Ti:Sapphire pulsed laser (800 nm, $\sim$150 fs, $\sim$70 μJ). The resulting pulse typically comprises one cycle of the electric field and has a duration of $\sim$1 ps and a frequency spectrum between 0.4 and 1.2 THz. We obtain the dielectric function $\hat{\epsilon}(\nu)$ from the change in amplitude (absorption) and delay (refraction) of the THz pulse propagated through the sample [19]. The frequency window of the generated THz pulses does not reach down to the maximum of the main Debye response of water at 20 GHz, but the high frequency wing of this response extends to THz frequencies. The depolarization of the main Debye mode can therefore be measured by THz-DR.

B.   fs-IR Pump-Probe

In the fs-IR pump probe experiment we excite and probe the OD stretch vibration of HDO molecules in isotopically diluted water with an ultrafast laser pulse tat is resonant with the $\nu = 0 \rightarrow 1$ transition (4 μm). The pulses are generated via frequency-conversion processes that are pumped with the output of a Ti:Sapphire 110 fs 800 nm pulsed laser (Hurricane, Spectra-Physics) [32]. The generated pulses have a central wavelength of 4 μm, a duration of 150 fs, and a pulse energy of 5 μJ. The pulses are used in a polarization-resolved pump-probe experiment. The excitation by the pump pulse labels a subset of water molecules that have their OD stretch transition dipole aligned preferentially in the direction of the pump polarization, thus creating an anisotropically excited ensemble. After a tunable delay, a probe pulse (20 nJ), with its polarization either parallel or perpendicular to the pump polarization, interrogates the sample. At short delay times after the excitation, the probe with its polarization parallel to the pump will give a larger signal than the perpendicular probe, due to the pump-induced anisotropy. With increasing delay times the excited ensemble will decay to an isotropic state in which both probe signals are identical. The time scale at which this happens is a measure for the characteristic time at which the molecules reorient in the liquid. The transient absorption spectra measured with the parallel probe ($\Delta\alpha_\parallel$) and the perpendicular probe ($\Delta\alpha_\perp$) for pump-probe delay times t are used to construct the anisotropy parameter $R(t)$,

$$R(t) = \frac{\Delta\alpha_\parallel(t) - \Delta\alpha_\perp(t)}{\Delta\alpha_\parallel(t) + 2\Delta\alpha_\perp(t)}, \tag{3}$$

The denominator represents the isotropic signal. In the expression for $R(t)$ all isotropic effects like the vibrational relaxation are divided out so that the dynamics of $R(t)$ represents the reorientation of the excited vibration only. For a sample consisting of a randomly oriented collection of dipolar oscillators the maximum anisotropy $R = 0.4$. For a pure sample of 4% D_2O in H_2O the anisotropy decays with a time constant of 2.5 ps [33].

Fs-IR and THz-DR measure intrinsically different observables [34, 35]. THz-DR is sensitive to the first-order time dipole-dipole correlation function, while fs-IR measures the second-order time-correlation function of the OD transition dipole orientation. In addition to that, while fs-IR measures the reorientation of - a labeled subset of - single molecules, THz-DR measures the macroscopic polarization to which also local field and dipole-dipole correlations contribute. For themain reorientation (Debye) component of bulk liquid water the ratio between the two timescales was found to be 3.4 [36].

C. Samples

The alkali-halide salts, guanidinium chloride (GndCl, see figure 1) and 1,1,3,3-tetramethylguanidine (TMG) were purchased from Sigma Aldrich. TMG is a strong base (pK$_a$ = 13.6) and was neutralized by adding a stoichiometric amount of hydrochloric acid to create the tetramethylguanidinium chloride (TMGndCl) salt. Figure 1 shows a graphical representation of the (tetramethyl)guanidinium cations. Solutions at different concentrations were prepared with a mixture of 4% D_2O in H_2O (Sigma Aldrich) as the solvent. The measured concentrations range from 0.25 to 4 m (mol/kg solvent) for the THz-DR experiment, and from 1 to 6 m for the fs-IR experiments. The deuterium atoms of D_2O exchange both with water to form HDO molecules and with the NH_2 groups of the guanidinium salts to form NHD. The resonance frequency of the thus formed ND is very close to that of the OD, but its cross section - which is entering quadratically in the pump-probe signal - is twice as small. In addition, for a 4 m GndCl solution the concentration of ND is 3 times lower than the OD concentration. Therefore the NHD groups will not contribute significantly to the pump probe signal. In the THz-DR experiment an Infrasil quartz cuvette was used with a pathlength of 103 ± 0.5 μm. In the fs-IR measurements we used two square CaF_2 windows (thickness 4 mm) with a 50 or 100 μm spacer in between. The concentrations of H_2O in the solutions are determined using a density meter (Mettler Toledo DM40).

III. EFFECTS OF IONS ON WATER DYNAMICS

A. THz Dielectric Relaxation

Figure 2A shows the imaginary part of the dielectric function $\hat{\epsilon}(\omega)$ for different salt solutions. The dielectric functions are calibrated using a reference salt solution with known dielectric properties that was measured in parallel. The solid lines in figure 2A are fits of equation (2) to the data. For stronger hydrated cations we observe a larger depolarization (decrease of S_1 in equation (1)). Figure 2B shows the depolarization caused by hydration shell water molecules that do not participate in dielectric relaxation for a series of concentrations. The depolarizations are corrected for the kinetic depolarization term [32], using conductivity values from the literature [13, 28–31]. The slope of the fitted lines represents the hydration number N_p, the number of (dipoles of) water molecules that show much slower orientational dynamics than bulk water due to the electrostatic interactions with the ions. The weakly hydrated cation cesium has a very small hydration number

6

($N_p \approx 0$), meaning that this ion hardly affects the orientational dynamics of water. For smaller cations (Na^+ or Li^+) or increasing cation charge (Mg^+) the slope becomes much larger, indicating a larger hydration number. In line with previous results [37], the anions show very little effect, as is demonstrated by the results for Cs_2SO_4 which combines the weakly hydrated cation Cs^+ with the strongly hydrated anion SO_4^{2-}.

B. fs-IR Pump-Probe

Figure 3 shows transient absorption spectra at different pump-probe delay times measured for a 4 mol/kg NaCl solution. The excitation of a few percent of the OD vibrations to the first excited state leads to transient spectra that consists of two main contributions. At frequencies >2450 cm^{-1} a bleaching signal is observed due to the bleaching of the ground state and stimulated emission out of the excited state. At frequencies <2450 cm^{-1} induced absorption from the first to the second excited state is observed. The latter absorption is red-shifted with respect to the fundamental transition because of the anharmonicity of the OD vibration. Vibrational relaxation from the first excited state to the ground state will lead to a decay of the transient spectral changes. At long delay times all OD oscillators have completely relaxed and the energy has become thermally equilibrated over the sample. From those times on the transient spectrum represents the effect of a small increase in temperature (by a few kelvin) on the absorption spectrum of the sample.

As the dissolution of NaCl introduces a blue-shift of the OD absorption band in the linear spectrum (figure 1), we model the isotropic data with two independent excited states representing the absorption of the bulk-like HDO:H$_2$O molecules and a blue-shifted absorption band of HDO molecules hydrating ions [38]. The results of the fit to the data obtained for a 4 mol/kg NaCl solution are shown in figure 3 and 4. The experimental spectra are well described by a sum of two spectral components centered around 2500 and 2530 cm^{-1}. The decay time of the blue-shifted component is 4.5 ps, which is considerably slower than the bulk-like component (1.8 ps). We assign the blue component to water solvating the chloride (OD$\cdots$Cl$^-$). It has been shown before that around chloride and most other halide ions the decay of the OD/OH-stretch excitation is much slower than in bulk liquid water [38, 39]. For a number of chloride solutions it was found that independent of the cation, a 30 cm^{-1} blue shifted component is present [38, 40, 41]. The blue-shift and the slower relaxation can be explained from the fact that the OD$\cdots$Cl$^-$ hydrogen bond is weaker than the average water-water hydrogen bond (OD$\cdots$O) [40]. In case of larger

7

halide anions the surface charge density is smaller, the hydrogen-bond even weaker and hence the blue-shift larger (for example $\sim$70 cm^{-1} in case of OD$\cdots$I$^-$, figure 1). Since all salt solutions under study with fs-IR contain either chloride or iodide, the same kinetic model is used for all fs-IR data shown in this paper.

We use the fitted spectra and their dynamics to correct the data for the ingrowth of the thermal difference spectrum in order to calculate the anisotropy decay of purely the excited OD oscillators. Since the vibrational lifetime of the OD$\cdots$Cl$^-$ component is different from that of the OD$\cdots$O component, we have to decompose the data such that we can determine the anisotropy decays of both components separately. The total difference transient spectra $D(t,\omega)$ is given by:

$$D(t,\omega) = \Delta\alpha_\parallel(t,\omega) - \Delta\alpha_\perp(t,\omega) = R_O(t,\omega)N_O(t)\sigma_O(\omega) + R_A(t,\omega)N_A(t)\sigma_A(\omega), \quad (4)$$

where $R_i(t,\omega)$ denotes the delay time-dependent anisotropy of the OD oscillators bound to other water molecules ($i = O$) or the anion ($i = A$) probed at frequency ω. $N_i(t)$ denotes the excited population at pump-probe delay time t and $\sigma_i(\omega)$ is the excited state spectrum of species OD$\cdots$O or OD$\cdots$A, obtained from the isotropic fit (figure 4). For most of the systems under study spectral diffusion is fast enough such that the anisotropy within one state can be treated as behaving uniformly, so that the frequency dependence of R_i can be neglected [39, 42]. This enables us to obtain the time dependent amplitude $R_i(t)N_i(t)$ for every time t by fitting the spectra $\sigma(\omega)$ of the different components to the difference transient spectrum $D(t,\omega)$. For every component i the time traces resulting from the decomposition contain the anisotropy decay $R_i(t)$ multiplied by the isotropic population decay $N_i(t)$. The latter is known from the isotropic fit and can thus be divided out. The anisotropy curves for the OD$\cdots$O, OD$\cdots$Cl$^-$ and OD$\cdots$I$^-$ components of 4 mol/kg solutions of NaCl and NaI are shown in figure 5A.

The anisotropy decay of the OD$\cdots$O species ($R_O(t)$) can be fitted well with a mono-exponential function with a time constant of $\approx$2.5 ps and thus resembles the dynamics observed for pure HDO:H$_2$O [33]. It should be noted that $R_O(t)$ also contains the dynamics of the water molecules in the hydration shell of the cations.

The anisotropy decay of anion bound OD groups ($R_A(t)$) shows a very different behavior compared to $R_O(t)$. Within the first few hundred femtoseconds an extremely rapid decay makes the anisotropy drop to about 75% of its theoretical maximum of 0.4, likely due to fast librational motions [43]. This contribution can be fitted separately for early delays with a mono-exponential

8

function with a time constant of 170±40 fs.

To interpret the behavior of $R_A(t)$ for different salts, we should take into consideration that the OD oscillators in the bulk exchange with those in the ion hydration shell. These exchange events occur on a time scale of ∼9 ps [44]. As a result, there will be oscillators that are initially excited as OD$\cdots$A$^-$, and that are probed after having rotated *out* of the anion hydration shell. Since their spectral response also changed, these oscillators are no longer contributing to $R_A(t)$. However, there are also oscillators that are excited as OD$\cdots$O and that are probed after having rotated into the anion hydration shell. This class of oscillators contributes to the spectral response of the OD$\cdots$A$^-$ component but will have lost almost all of their directionality in the exchange event, thereby lowering $R_A(t)$.

We model the anisotropy of the anion-bound water by assuming a bi-exponential form for the intrinsic anisotropy $R_A^{intr}(t)$, i.e. the anisotropy of the ion hydration shell in case there would be *no* exchange [45]:

$$R_A^{intr}(t) = R_0 \left[(1 - B_0)e^{-k_1^A t} + B_0 e^{-k_2^A t} \right] \tag{5}$$

Here R_0 is the initial amplitude, B_0 a proportionality factor between the two exponentials and k_1^A and k_2^A the rates of the reorientation processes. The initial drop due to librational motions is here neglected, as we only consider the data after 0.5 ps in the fit. We include exchange effects by modeling the population dynamics of OD groups that remain hydrogen bonded and the rotated-in OD groups separately using the exchange rate and the vibrational decay rate [45]. It is not possible to determine the time scale of the exchange for chloride and iodide solutions from our experiments because the OD$\cdots$O, OD$\cdots$Cl$^-$ and OD$\cdots$I$^-$ strongly overlap. Therefore we fixed the exchange time constant to 9 ps, as found by Gaffney for perchlorate solutions [44]. Rotating into the anion hydration shell involves a jump over an angle of ∼55 degrees [44], making the OD-oscillators to loose their orientation completely in the event. The solid lines in figure 5A represent the intrinsic $R_A^{intr}(t)$ for the NaCl and NaI solutions that follows from a fit to the data including the exchange effects. For both NaCl and NaI we find $(k_1^A)^{-1}$=2±0.3 ps and $(k_2^A)^{-1}$=9±1 ps. The 2±0.3 ps component has a quite large amplitude. Although $R_A(t)$ only represents the reorientation of anion bound OD groups, it not only depends on the nature of the anion but also on the nature of the cation. In Figure 6 we compare the dynamics of $R_{A=Cl}(t)$ for chloride salts with a strongly hydrated cation (NaCl) and a weakly hydrated cation (CsCl). We observe that the 2 ps decay component of $R_{Cl}(t)$ has a smaller amplitude for a solution of NaCl than for a solution of CsCl. In figure 5B the relative amplitude of the slow component of $R_A^{intr}(t)$ (one minus the fraction

9

of the fast component) is shown as a function of concentration. This amplitude increases with concentration and is larger for NaCl than for NaI.

C. Discussion

1. *Effect of cations*

Figure 2 shows that the effect of salts on the orientation dynamics of the water dipoles, as measured with THz-DR, is dominated by the nature of the cation. The fraction of slow water is larger going from CsCl to NaCl to $MgCl_2$, which can be explained from the increase of the surface charge density of the cation. When the surface charge density becomes larger, the electric field exerted on the surrounding water molecules also increases. Mg^{2+} is doubly charged and has an even smaller radius than Na^+, making its alignment effect on the water dipoles very strong. This results in the observation of a large fraction of slow water for solutions containing Mg^{2+}.

Previous fs-IR experiments showed that cations have a relatively small effect on the reorientation of the water hydroxyl groups. The anisotropy decay of solutions of $Mg(ClO_4)_2$ is observed to be hardly different from that of pure water [7], meaning that the strong electric field exerted by Mg^{2+} hardly influences the orientational mobility of the hydroxyl groups. Cations thus primarily limit the reorientation of the water dipoles but leave the reorientation of the hydroxyl groups largely unaffected.

These findings point at the following picture of the cation hydration shell. The positive charge of a cation attracts the negatively charged oxygen atom of the water molecule and repels the positively charged hydrogen atoms, thereby fixing the dipole moment of the water molecule in a radial direction [8]. In this configuration the OD/OH groups of the water molecules remain relatively free to reorient. The dynamics of the OD/OH groups will thus not be strongly different from the dynamics of bulk liquid water. Of course, one could argue that the restricted rotation in a cone (with the dipole moment as the primary axis) constitutes a limitation compared to the case of bulk water. However, a water molecule in the bulk experiences a strong restriction in its rotational mobility resulting from the hydrogen bonds that it accepts from other water molecules. These accepted hydrogen bonds fix the positions of the lone pairs of the oxygen atom of the reorienting water molecule, thus limiting the orientational space of the hydroxyl groups at the other side of the molecule. For a water molecule with its oxygen atom adjacent to a cation this limitation is

10

less severe. The two restrictions (cone-like reorientation and fixing of the lone pairs) may have a similar effect on the orientational mobility of the water molecule, thus making the reorientation rates of hydroxyl groups in the cation hydration shell and in bulk quite similar.

2. *Effect of anions*

The effect of anions on the orientational mobility of the water dipoles probed with THz-DR is quite small, as is illustrated by the weak effect of Cs_2SO_4 in Figure 2. The fact that anions do not fix the water dipoles shows that the interactions of anions with water is not purely electrostatic in nature. Otherwise, the effects of cations and anions should have been quite similar, and a strongly hydrated anion would have fixed its surrounding water dipoles in a similar manner (but opposite direction) as a strongly hydrated cation.

Fs-IR probes the transition dipole of the OD-stretch vibration, and thus measures the reorientation dynamics of the hydroxyl groups of the water molecules. In this case the effects of salts on the water dynamics are dominated by the nature of the anion. If the anion strongly binds the water molecules, a corresponding large fraction of water molecules is observed for which the orientational dynamics of the OH groups is slow [8].

There exists an interesting asymmetry in the effects of anions and cations on the dynamics of water. This asymmetry is due to the fact that most anions accept hydrogen bonds from the OH groups of the solvating water molecules. Hydrogen bonds have as a special property that they are much stronger in case the OH bond is aligned with the $O \cdots A^-$ coordinate [46]. The formation of such a directional hydrogen bond prevents a configuration in which the electrostatic interaction would have been optimized. If the interaction between the anion and water would have been purely electrostatic, the anion would have been closest to the middle of the two hydrogen atoms of the water molecules, and the OH groups would thus be positioned in a straddling configuration. However, in such a configuration the OH bonds make a quite large angle with the $O \cdots A^-$ coordinate and the hydrogen-bond interaction would be very weak. It is thus energetically favorable to form a directional $OH \cdots A^-$ with only one of the OH groups of the water molecule. The other OH group points away from the anion and will form a hydrogen bond to another water molecule. The directional character of this hydrogen bond limits the mobility of the bonded OH group, but leaves the other OH group and the dipole moment of the water molecule relatively free to reorient.

The fast reorientation process with a time constant of ~ 2 ps that we find for $R_A(t)$ can be as-

11

signed to a wobbling motion of the OD groups that keep their hydrogen bond with the anion intact. The HOD molecules that donate these OD groups can form up to three hydrogen bonds to water molecules outside the anion hydration shell. The reorganization of the hydrogen-bond network outside the first hydration shell is therefore reflected in the orientation of the HOD molecule and thus the wobbling motion of the anion bound OD group. The fitted fast time constant of 2 ± 0.3 ps is in good agreement with this interpretation. For larger anions, for example I^-, the angular spread over which OD groups have the freedom to wobble is larger (figure 7), and thus the amplitude of the fast component is larger (figure 5, note that the fraction of the slow component is shown). Since the maximal anisotropy decay due to the wobbling motion is determined by the cone angle, any residual anisotropy will have to decay through other processes like the reorganization of the hydration shell or the reorientation of the complete anion hydration structure. The time constant that we find for this process is 9 ± 1 ps, in agreement with previous studies on salt solutions, in which only the dynamics at longer delays was considered [38]. This time constant should not be confused with the time constant of exchange, which is coincidentally also 9 ps.

The presence of a quite large wobbling component in the orientational dynamics of the OD groups bonded to the halide anions will enlarge the orientational space for the dipole moment of the water molecules to which the OD groups belong. Hence, the wobbling component forms part of the reason why halide anions have a negligible effect on the orientational mobility of water dipoles. In fact, the average orientational mobility of the water dipoles has been observed to be even somewhat faster for solutions of halide anions than for bulk water [37], which may be due to the fact that the wobbling motion in the hydration shell of the halide anions shows a somewhat shorter time constant than the reorientation time of bulk liquid water.

3.   Cooperative effects of cations and anions

Although cations primarily affect the reorientation of the water dipoles and anions the reorientation of the water hydroxyl groups, there are indications of cooperative effects. For instance, the nature of the cation influences the reorientation of the water molecules in the anion hydration shell (figure 6). Probably, the electric field exerted by the cation restricts the cone over which the anion-bound OD groups can wobble. This effect increases with increasing charge density of the cation, i.e. in the series $Cs^+ < Na^+ < Li^+ < Mg^{2+}$.

The cooperative effect of cations and anions on the dynamics of water increases with increasing

12

hydration strength of both ions. For MgSO$_4$ solutions the hydration number is ∼18 both in dielectric relaxation and in femtosecond IR measurements [8]. This large hydration number implies that the hydration structures must extent well beyond the first hydration shells of the ions. The formation of the extended rigid hydration structures probably arise as a result of the combination of a strong fixing of the dipole vectors by the cations and a strong fixing of the direction of the hydroxyl groups by the anions. The Mg^{2+} and SO$_4^{2-}$ ions thus cooperate in impeding the water mobility over relatively long ranges and probably induce the formation of a locked hydrogen-bonded structure of water molecules in between the ions. This latter picture is in line with the observation that solutions of strongly hydrated ions, like MgSO$_4$, give rise to the formation of solvent-separated ion pairs [47].

IV. HYDROPHOBIC EFFECTS ON WATER DYNAMICS

We investigate the combined effects of electrostatic and hydrophobic interactions by comparing the effects of guanidinium chloride (GndCl) and tetramethylguanidinium chloride (TMGndCl) on the dynamics of water.

A. THz Dielectric Relaxation

In figure 8 we show the imaginary part of the dielectric function measured for different concentrations of GndCl and TMGndCl. TMGndCl shows a much stronger depolarization effect than GndCl. This cannot be due to electrostatic alignment of the water molecules in the solvation shell of the cation, since the electric field exerted by the TMGnd$^+$ cation is not stronger than the field exerted by the Gnd$^+$ cation. More likely, a large fraction of water in TMGndCl solutions reorients slowly because of the presence of the hydrophobic methyl groups, as has been observed before for other amphiphilic solutes [19, 48]. For these water molecules the frequency response has shifted to lower frequencies. We model these water molecules with an additional Debye mode, resulting in the model function:

$$\hat{\epsilon}(\nu) = \frac{S_{slow}}{1 + 2\pi i \nu \tau_{\text{slow}}} + \frac{S_{bulk}}{1 + 2\pi i \nu \tau_{\text{bulk}}} + \frac{S_{fast}}{1 + 2\pi i \nu \tau_{\text{fast}}} + \frac{\sigma}{2\pi i \epsilon_0 \nu} + \epsilon_\infty. \tag{6}$$

As pointed out in the experimental section, the THz-DR experiment is not very sensitive to the frequency dependence of the dielectric relaxation modes that peak at much lower frequencies.

13

The THz-DR experiment is mainly sensitive to these modes, as a decrease in the amplitude leads to depolarization. Hence in fitting the observed dielectric response of the TMGndCl, we fix the View Online values for τ_{slow} of the slow water mode and τ_{bulk} of the bulk water to the parameters found for TMU in the GHz regime [19]. The THz-DR experiment is sensitive to the amplitude of these modes. The fits to the data are presented as the solid lines in figures 8.

After correcting for dilution effects and the kinetic depolarization, we obtain the values of the slow water fractions for the different solutions, shown in figure 12A. For comparison we also show the slow fractions observed for TMU at the same concentrations [19].

B. fs-IR Pump-Probe

The isotropic transient absorption data obtained for guanidinium chloride (GndCl) and tetramethylguanidinium chloride (TMGndCl) were modeled according to the description in section III B. The transient spectra of GndCl showed the presence of a third spectral component (in addition to the OD$\cdots$O and OD$\cdots$Cl$^-$ components) on the red side of the OD$\cdots$O spectrum (<2470 cm^{-1}) with a very fast vibrational decay, possibly due to coupling to vibrational modes in the guanidinium cation [12, 49]. This component will be subject of a future study. In the present study we minimize the contribution of this fast component by using a pump-probe frequency centered around 2525 cm^{-1}.

Figure 9 shows the total anisotropy measured for solutions of GndCl and TMGndCl of different concentrations. The curves shown in figure 9 represent the averaged reorientation behavior of all OD$\cdots$O and OD$\cdots$Cl$^-$ groups in solution, weighted by their respective time-dependent populations. For the GndCl solutions the anisotropy decays are observed to be only slightly different from the anisotropy decays of pure HDO:H$_2$O. In contrast, the anisotropy curves of the TMGndCl solutions show a much slower decay, indicating that a large amount of the water molecules show very slow orientational dynamics. The slowing down effect strongly increases with concentration.

The dynamics of the OD$\cdots$O and OD$\cdots$Cl$^-$ component of the TMGndCl solutions cannot be determined using the same analysis method that was used for the alkali-halide salts, as this analysis requires the anisotropy dynamics to be frequency independent within the two components. This condition is fulfilled for the alkali-halide solutions, because these solutions show quite fast spectral diffusion. However, for TMGndCl we observe a frequency dependence of the anisotropy that persists at longer delays, as shown in figure 10, indicating that the solution is heterogeneous and

that the spectral diffusion is quite slow. Hence $R_A(t, \omega)$ should be taken dependent on frequency in equation 4. To fit the data we use the following functional forms for the anisotropy values of the two components. For $R_O(t)$ we take a bi-exponential function representing bulk water and water with slower dynamics due to the presence of hydrophobic groups,

$$R_O(t) = R_0 \left[(1 - A)e^{-k_1^O t} + Ae^{-k_2^O t} \right] \tag{7}$$

where A is the fraction of water with slower dynamics, k_1^O the bulk water reorientation rate and k_2^O the reorientation rate of the water with slower dynamics. We fit the data starting at 0.5 ps, thus neglecting any contribution due to fast libration motions.

$R_{Cl}(t)$ was already found to possess a fast and a slow component (equation (5)). The dynamics of the fast (wobbling) component is governed by the hydrogen-bond dynamics of the surroundings. Hence, this component will be slowed down as a result of the presence of the hydrophobic molecular groups in solution. In addition, there is a persistent frequency dependence of the relative amplitudes $1 - B_0$ of the wobbling component and B_0 of the slow component because the spectral diffusion is slow. The functional form of the anisotropy parameter for chloride-bound water is thus:

$$R_{Cl}(\omega, t) = R_0 \left[(1 - B_\omega) \left((1 - A)e^{-k_1^{Cl} t} + Ae^{-k_2^{Cl} t} \right) + B_\omega e^{-k_3^{Cl} t} \right] \tag{8}$$

where the rates k_1^{Cl} and k_2^{Cl} are analogous to the rates from equation 7. The relative amplitude between the fast and slow component B_0 is, due to the strong inhomogeneous character of the solution, replaced by B_ω, for which we take a linear frequency dependence. The amplitudes of the wobbling motion (~ 2 ps) and the slower rotational diffusion (~ 9 ps, not the exchange) thus show an opposite linear dependence on frequency that does not depend on the delay time. We do not include the effects of the exchange between the bulk and the hydration shell in the anisotropy dynamics of the OD$\cdots$Cl$^-$ component. This exchange is expected to be quite slow in view of the high viscosity of the samples and the slow spectral dynamics of the TMGndCl solutions. In work soon to be published we treat this analysis in more detail [50].

To limit the free parameters in the fit, we fix $(k_1^O)^{-1}$ to a value of 2.5 ps, as observed for a pure 4% D$_2$O in H$_2$O sample [33]. Furthermore we fix $(k_1^{Cl})^{-1}$ to 2 ps and the amplitude of B_ω at 2530 cm^{-1} to the value found for the CsCl solution of the same concentration [45]. The rates k_2^{Cl} and k_3^{Cl} in equation 8 both represent a slow timescale and we assume these to be the same. This is of course not necessarily the case, but as we can only measure the anisotropy dynamics up to 10 ps, we cannot distinguish between relaxation time constants that are similar to or larger than

10 ps. The fitted values of $k_2^{Cl} = k_3^{Cl}$ lie in the range of 30 to 40 ps. The amplitude of the slow component of $R_{Cl}(t)$ is thus the sum of the slow component resulting from the binding to the anion and the fraction of the fast (wobbling) component that is slowed down as a result of the hydration of the hydrophobic molecular groups. Consistent with the THz-DR analysis, we fix k_2^O in $R_O(t)$ to the values found for TMU with GHz-DR [19], taking into account the conversion factor ~ 3.4 discussed at the end of section II A. The results of the fits are presented as the solid lines in figure 11 and the slow water fractions calculated from the fitted amplitudes A are plotted in figure 12B.

C.   Discussion

The addition of GndCl to water is observed to have a very small effect on the reorientation dynamics of the water molecules. Guanidinium is a rather large cation which means that the charge density of the positive charge will be rather low. Hence, the electrostatic interaction between water and this ion will be rather weak. The interaction of water with guanidinium will be dominated by hydrogen bonding to the NH$_2$ groups. These hydrogen-bond interactions will be quite similar to the hydrogen bonds between water molecules and the hydrogen bonds between water and urea (CH$_4$N$_2$O) [13, 14]. Urea was also observed to show very little effect on the reorientation dynamics of water. Apparently, the similarity of the hydrogen-bond interactions to water allow the water molecules to reorient with a similar rate as is observed in bulk liquid water. The small slowing down of the total anisotropy decay observed for solutions of GndCl, as shown in figure 9A, can be fully assigned to the presence of the chloride anion. Since Cl$^-$ anions bind the solvating water molecules by making a hydrogen bond to their OH/OD groups, the dipole moments of these water molecules remain quite free in their reorientation, as was discussed in the previous section. The water dipole moments thus show a similar mobility as in bulk water, as is indeed observed in the THz-DR measurements (figure 12A).

TMGndCl is observed to have a large effect on the dynamics of water. The fs-IR measurements show a strong slowing down of the water dynamics in both the OD$\cdots$O and the OD$\cdots$Cl$^-$ component. The increase of the slow component in the chloride-bound water compared to GndCl can be completely ascribed to the effects of the hydrophobic molecular groups of TMGnd$^+$ on the dynamics of the wobbling component of the chloride-bound OD groups. The THz-DR results show a similar slowing down effect of the water dynamics as is observed in the fs-IR experiments, which indicates that the TMGnd$^+$ cation affects the dynamics of the OD groups and the water dipole

moments in a similar manner. For solutions of TMU it was also observed that the slowing down effect is quite similar in dielectric relaxation and in femtosecond mid-infrared measurements [19]. It is illustrative to compare the results obtained for TMGndCl with the results obtained for solutions of TMU at the same concentration, as TMU also possesses four methyl groups in a similar configuration as the $TMGnd^+$ cation. The THz-DR data of TMGndCl agree very well with the results of TMU (figure 12), confirming that the effects of $TMGnd^+$ and TMU on the dynamics of water are completely dominated by the methyl groups.

In figure 12B the slow water fraction of the TMU and TMGndCl solutions shows a saturation effect that has its origin in overlapping hydration shells and aggregation. TMU is known to aggregate at higher concentrations [19, 51, 52]. This figure shows that the aggregation effect for the $TMGnd^+$ cation is quite similar as for TMU, at least up to concentrations of 4 m. This is somewhat surprising because the positive charge of the $TMGnd^+$ cations is expected to disfavor aggregation. Apparently, the electrostatic effects of this charge are very weak, as is also demonstrated by the very weak effects of the Gnd^+ cation on the dynamics of water.

In recent two-dimensional infrared (2D-IR) spectroscopy studies it was found that water molecules show very slow spectral dynamics around the hydrophobic groups of tertiary butylalcohol (TBA), trimethylamine-N-oxide (TMAO) and (TMU) [53, 54]. The fraction of water showing slow spectral diffusion was found to be highly correlated to the fraction of water showing slow reorientation dynamics [54]. This correlation points at a common origin. The molecular reorientation of water involves a jump mechanism in which the hydrogen atom of the reorienting hydroxyl group forms a bifurcated hydrogen bond to the oxygen atoms of two nearby water molecules [23, 55, 56]. The evolution from a linear hydrogen bond to the bifurcated transition state is accompanied by a large change in vibrational frequency and thus leads to strong spectral diffusion, irrespective of whether this evolution leads to a new hydrogen bond and thus reorientation (successful switch) or to the restoring of the original hydrogen bond (unsuccessful switch). The correlated slowing down of the spectral diffusion and the reorientation indicates that water near hydrophobic groups is strongly hindered in its evolution to a bifurcated hydrogen bond structure. A possible explanation for this observation is that the hydrophobic solute methyl groups fill up the cavities of the hydrogen bond network of water, thereby preventing the local collapses of the network that are required for the formation of bifurcated hydrogen bonds.

In NMR studies it is also observed that hydrophobic molecular groups have a strong effect on the reorientation dynamics of liquid water that increases with increasing size of the hydrophobic

group [57–60]. For instance, in the NMR study by Shimizu et al. [59], the slowing down of the water reorientation dynamics was found to scale with the number of substituted methyl groups of the urea molecule, urea showing only a negligible effect and TMU the strongest effect. In the same study GndCl was also found to have a negligible effect on the reorientation dynamics of water [59], in line with the present observations. The reorientation and spectral diffusion dynamics of water in solutions of amphiphiles have also been studied with classical molecular dynamics simulations [52, 61, 62]. In these studies a slowing down of the reorientation and spectral diffusion of the water molecules around the hydrophobic groups is found, but not to the extent as is observed in the fs-IR and the 2D-IR experiments.

In order to relate the effects of GndCl and TMGndCl on the dynamics of water to their role in the denaturation of proteins, we measured the fraction of unfolded Photoactive Yellow Protein (PYP) as a function of concentration GndCl, TMGndCl, urea and TMU. The measurements, of which the results are shown in figure 13, were performed according to the procedure described in Ref. [63] at pH 7 (using a potassium phosphate buffer). GndCl is clearly most effective, as it completely unfolds all PYP at a concentration of 3.5 mol/l. Urea is not only the least effective, its shallow slope indicates that more urea molecules per protein are needed for the denaturation process. These results indicate that the mechanisms for denaturation by GndCl and urea differ.

When the four hydrogen atoms of urea are replaced by methyl groups to form TMU, the effectiveness in denaturing PYP becomes strongly enhanced. One may expect the same enhancement for TMGndCl relative to GndCl, but TMGndCl is less effective than GndCl and shows a similar denaturation behavior as TMU. The denaturation mechanisms of urea and GndCl compounds appear to be completely replaced by denaturation effects associated with the methyl groups of TMU and TMGndCl. As TMGndCl and TMU also show a quite similar effect on the dynamics of water, the similar denaturation effect of TMGndCl and TMU may well be related to the hydrophobic hydration of their methyl groups.

V.   CONCLUSIONS

We studied the effects of ions and hydrophobic molecular groups on the reorientation dynamics of water using THz dielectric relaxation (THz-DR) and polarization-resolved femtosecond mid-infrared spectroscopy (fs-IR). THz-DR probes the reorientation of the water dipole moments while

fs-IR probes the reorientation of the water OH/OD groups.

We find that cations primarily slow down the reorientation dynamics of the water dipole moments. This effect increases with decreasing size and increasing charge of the cation. Anions primarily slow down the reorientation dynamics of the water OH/OD groups. Most anions form a directional hydrogen bond with one of the OH/OD groups of the solvating water molecules.

The reorientation of OD groups that are hydrogen bonded to the halide anions Cl^- and I^- is found to consist of two components: a fast component with a time constant of 2 ± 0.3 ps and a slow component with a time constant of 9 ± 1 ps. The fast component represents a wobbling motion of the OD groups that keeps the hydrogen bond intact. The dynamics of this motion are governed by the dynamics of the water hydrogen-bond network outside the anion hydration shell. The slow component is associated with the diffusion of OD groups over the surface of the anion and/or with the reorientation of the complete anion hydration structure.

The amplitude of the wobbling motion increases with increasing size of the anion and also depends on the nature of the cation. For a strongly hydrated cation like sodium, the wobbling cone is restricted to smaller angles. When very strongly hydrated anions and cations are combined, as in a solution of $MgSO_4$, the restrictions on the wobbling cone angle and the water dipole moments are large enough to lock water molecules in both degrees of freedom outside the first solvation shells.

A comparison of the dynamics of water molecules in solutions of guanidinium chloride (GndCl) and tetramethyl guanidinium chloride (TMGndCl) salts shows that the effect on the dynamics of water are dominated by the hydrophobic methyl groups of the TMGnd cation. For GndCl solutions there is a small slow component in the reorientation dynamics associated with water molecules that are hydrogen bonded to the Cl^- anion. The guanidinium ion has no effect on the reorientation dynamics of water. The four methyl groups of $TMGnd^+$ lead to a strong slowing down of the reorientation dynamics of water, that is quite similar to what is observed for solutions of tetramethylurea (TMU). The water molecules that form hydrogen bonds to Cl^- show, in addition to the anionic effect, a strong slowing down of their wobbling motion due to the nearby presence of the hydrophobic $TMGnd^+$ cations.

Finally, we put these results in the perspective of the capabilities of GndCl, TMGndCl, urea and TMU to denature proteins. While urea and GndCl have very different mechanisms of denaturation, TMGndCl and TMU both show very similar behavior. As TMGndCl and TMU also show a similar effect on the dynamics of water, the denaturation mechanism of TMGndCl and TMU may well be

associated with their hydrophobic effect on the dynamics of water.

[View Online](#)

[1] Hofmeister, F. *Arch. Exp. Pathol. Pharmakol* **24**, 247–260 (1888).

[2] Marcus, Y. *Chem. Rev.* **109**, 1346–1370 (2009).

[3] Smith, J. D., Saykally, R. J., and Geissler, P. L. *J. Am. Chem. Soc.* **129**, 13847–13856 (2007).

[4] Mancinelli, R., Botti, A., Bruni, F., Ricci, M. A., and Soper, A. K. *J. Phys. Chem. B* **111**, 13570–13577 (2007).

[5] Schmidt, D. A., Birer, O., Funkner, S., Born, B. P., Gnanasekaran, R., Schwaab, G. W., Leitner, D. M., and Havenith, M. *J. Am. Chem. Soc.* **131**, 18512–18517 (2009).

[6] Lin, Y. A., Auer, B. M., and Skinner, J. L. *J. Chem. Phys* **131**, 144511 (2009).

[7] Omta, A. W., Kropman, M. F., Woutersen, S., and Bakker, H. J. *Science* **301**, 347–349 (2003).

[8] Tielrooij, K. J., Garcia-Araez, N., Bonn, M., and Bakker, H. J. *Science* **328**, 1006–1009 (2010).

[9] Rashid, F., Sharma, S., and Bano, B. *The Protein Journal* **24**, 283–292 (2005).

[10] Camilloni, C., Rocco, A. G., Eberini, I., Gianazza, E., Broglia, R. A., and Tiana, G. *Biophys. J.* **94**, 4654–4661 (2008).

[11] Lim, W. K., Rosgen, J., and Englander, S. W. *PNAS* **106**, 2595–2600 (2009).

[12] Scott, J., Nucci, N. V., and Vanderkooi, J. M. *J. Phys. Chem. A* **112**, 10939–10948 (2008).

[13] Hunger, J., Niedermayer, S., Buchner, R., and Hefter, G. *J. Phys. Chem. B* **114**, 13617–13627 (2010).

[14] Mason, P. E., Neilson, G. W., Dempsey, C. E., Barnes, A. C., and Cruickshank, J. M. *PNAS* **100**, 4557–4561 (2003).

[15] Das, A. and Mukhopadhyay, C. *J. Phys. Chem. B* **113**, 12816–12824 (2009).

[16] Mason, P. A., Brady, J. W., Neilson, G. W., and Dempsey, C. E. *Biophys. J.* **93**, L4–L6 (2007).

[17] Stumpe, M. C. and Grubmuller, H. *J. Am. Chem. Soc.* **129**, 16126–16131 (2007).

[18] Wei, H., Fan, Y., and Gao, Y. *J. Phys. Chem. B* **114**, 557–568 (2010). View Online

[19] Tielrooij, K. J., Hunger, J., Buchner, R., Bonn, M., and Bakker, H. J. *J. Am. Chem. Soc.* **132**, 15671–15678 (2010).

[20] Bakker, H. J. and Skinner, J. L. *Chem. Rev.* **110**, 1498–1514 (2010).

[21] Heugen, U., Schwaab, G., Bründermann, E., Heyden, M., Leitner, D. M., and Havenith, M. *PNAS* **103**, 12301–12306 (2006).

[22] Fukasawa, T., Sato, T., Watanabe, J., Hama, Y., Kunz, W., and Buchner, R. *Phys. Rev. Lett.* **95**, 197802 (2005).

[23] Laage, D. and Hynes, J. T. *Science* **311**, 832–835 (2006).

[24] Yada, H., Nagai, M., and Tanaka, K. *Chem. Phys. Lett* **464**, 166–170 (2008).

[25] Fecko, C. J., Eaves, J. D., and Tokmakoff, A. J. *J. Chem. Phys* **117**, 1139–1154 (2002).

[26] Turton, D. A., Hunger, J., Hefter, G., Buchner, R., and Wynne, K. *J. Chem. Phys* **128**, 161102 (2008).

[27] Zasetsky, A. Y. *Phys. Rev. Lett.* **107**, 117601 (2011).

[28] Bianchi, H., Corti, H. R., and Fernandez-Prini, R. *J. Sol. Chem.* **17**, 1059–1065 (1988).

[29] Buchner, R., Capewell, S. G., Hefter, G., and May, P. M. *J. Phys. Chem. B* **103**, 1185–1192 (1999).

[30] Chen, T., Hefter, G., and Buchner, R. *J. Phys. Chem. A* **107**, 4025–4031 (2003).

[31] Wachter, W., Fernandez, S., Buchner, R., and Hefter, G. *J. Phys. Chem. B* **111**, 9010–9017 (2007).

[32] Tielrooij, K. J., van der Post, S. T., Hunger, J., Bonn, M., and Bakker, H. J. *J. Phys. Chem. B* **115**, 12638–12647 (2011).

[33] Rezus, Y. L. A. and Bakker, H. J. *J. Chem. Phys* **123**, 114502 (2005).

[34] Böttcher, C. *Theory of Electrical Polarization Vol. I.* Elsevier (Amsterdam), (1973).

[35] Böttcher, C. *Theory of Electrical Polarization Vol. II.* Elsevier (Amsterdam), (1978).

[36] Tielrooij, K. J., Petersen, C., Rezus, Y. L. A., and Bakker, H. J. *Chem. Phys. Lett* **471**, 71–74 (2009).

[37] Wachter, W., Kunz, W., and Buchner, R. *J. Phys. Chem. A* **109**, 8675–8683 (2005).

[38] Kropman, M. F. and Bakker, H. J. *Science* **291**, 2118–2120 (2001).

[39] Park, S. and Fayer, M. D. *PNAS* **104**, 16731–16738 (2007).

[40] Bergstrom, P. A., Lindgren, J., and Kristiansson, O. *J. Phys. Chem.* **95**, 8575–8580 (1991).

[41] Kropman, M. F. and Bakker, H. J. *J. Am. Chem. Soc.* **126**(29), 9135–9141 July (2004).

[42] Roberts, S. T., Loparo, J. J., and Tokmakoff, A. *J. Chem. Phys* **125**, 084502 (2006).

[43] Nigro, B., Re, S., Laage, D., Rey, R., and Hynes, J. T. *J. Phys. Chem. A* **110**, 11237–11243 (2006).

[44] Gaffney, K. J., Ji, M., Odelius, M., Park, S., and Sun, Z. *Chem. Phys. Lett* **504**, 1–6 (2011).

[45] van der Post, S. T. and Bakker, H. J. *Phys. Chem. Chem. Phys.* **14**, 6280–6288 (2012).   View Online

[46] Moller, K. B., Rey, R., and Hynes, J. T. *J. Phys. Chem. A* **108**, 1275–1289 (2004).

[47] Buchner, R., Chen, T., and Hefter, G. *J. Phys. Chem. B* **108**, 2365–2375 (2004).

[48] Buchner, R., Hölzl, C., Stauber, J., and Barthel, J. *Phys. Chem. Chem. Phys.* **4**, 2169–2179 (2002).

[49] Vorobyev, D. Y., Kuo, C. H., Kuroda, D. G., Scott, J. N., Vanderkooi, J. M., and Hochstrasser, R. M. *J. Phys. Chem. B* **114**, 2944–2953 (2010).

[50] van der Post, S. T., Scheidelaar, S., and Bakker, H. J. To be published.

[51] Almasy, L., Lenb, A., Szkelyb, N. K., and Pletilc, J. *Fluid Phase Equilibria* **257**, 114–119 (2007).

[52] Stirnemann, G., Sterpone, F., and Laage, D. *J. Phys. Chem. B* **115**, 3254–3262 (2011).

[53] Bakulin, A. A., Liang, C., la Cour Jansen, T., Wiersma, D. A., Bakker, H. J., and Pshenichnikov, M. S. *Accounts of Chemical Research* **42**, 1229–1238 (2009).

[54] Bakulin, A. A., Pshenichnikov, M. S., Bakker, H. J., and Petersen, C. *J. Phys. Chem. A* **115**, 1821–1829 (2011).

[55] Loparo, J. J., Roberts, S. T., and Tokmakoff, A. *J. Chem. Phys* **125**, 194522 (2006).

[56] Bakker, H. J., Rezus, Y. L. A., and Timmer, R. L. A. *J. Phys. Chem. A* **112**, 11523–11534 (2008).

[57] Ishihara, Y., Okouchi, S., and Uedaira, H. *J. Chem. Soc. Faraday Trans.* **93**, 3337–3342 (1997).

[58] Fumino, K., Yukiyasu, K., Shimizu, A., and Taniguchi, Y. *J. Mol. Liq.* **75**, 1–12 (1998).

[59] Shimizu, A., Fumino, K., Yukiyasu, K., and Taniguchi, Y. *J. Mol. Liq.* **85**, 269–278 (2000).

[60] Qvist, J. and Halle, B. *J. Am. Chem. Soc.* **130**, 10345 (2008).

[61] Laage, D., Stirnemann, G., and Hynes, J. T. *J. Phys. Chem. B* **113**, 2428–2435 (2009).

[62] Stirnemann, G., Hynes, J. T., and Laage, D. *J. Phys. Chem. B* **114**, 3052–3059 (2010).

[63] Lee, B. C., Kumauchi, M., and Hoff, W. D. *Journal of Biological Chemistry* **285**, 12579–12586 (2010).

[64] Rezus, Y. L. A. and Bakker, H. J. *J. Phys. Chem. A* **112**, 2355–2361 (2008).
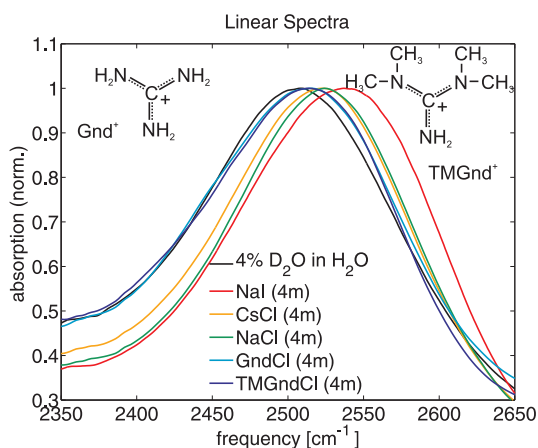
VI. FIGURES

FIG. 1: Linear absorption spectra in the region of the OD stretch vibration for concentrated solutions of the measured salts and pure 4% D_2O in H_2O.
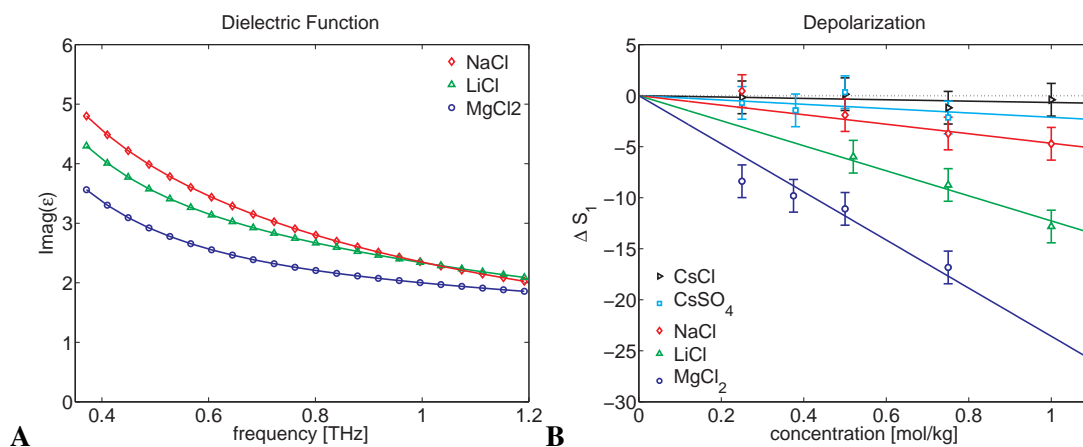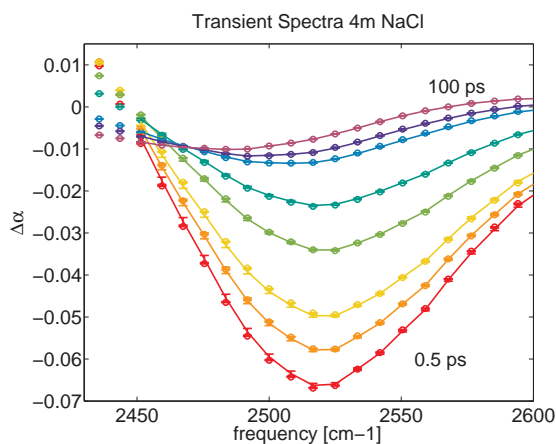

FIG. 2: (**A**) The imaginary part of the dielectric function measured for different salts. (**B**) The fraction of slow water deduced from the depolarization as a function of concentration for a number of salts. The weakly hydrated cesium hardly affects the dynamics of water, in contrast to the strongly hydrated magnesium.

23

FIG. 3: Transient absorption spectra at different delay times for a 4 mol/kg NaCl solution. The solid lines are the results from the fit to the model described in the text.
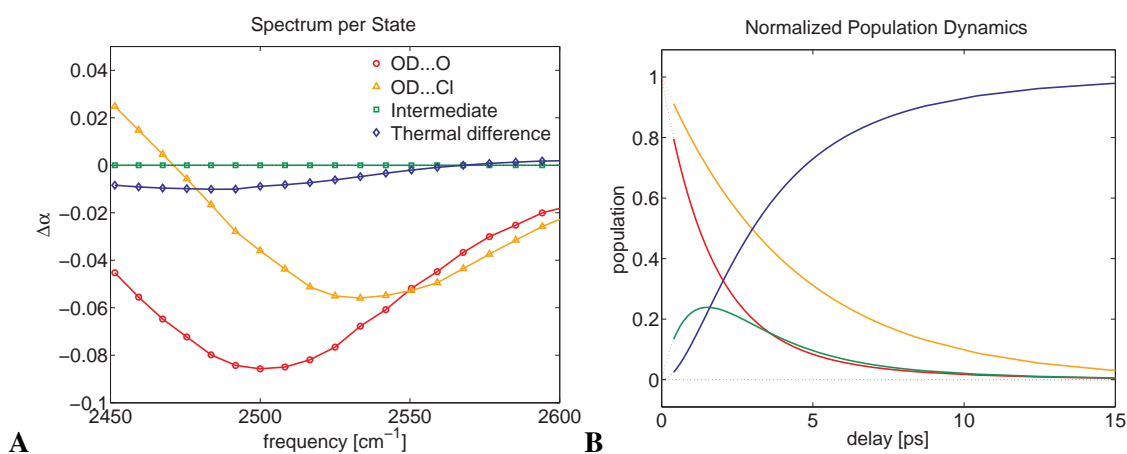
FIG. 4: (**A**) Spectral components obtained from the transient absorption spectra presented in figure 3. The response of the OD groups bound to the chloride is blue-shifted with respect to the OD$\cdots$O band. The intermediate state (squares) accounts for a slightly delayed ingrowth of the heat and has no associated spectrum. (**B**) Time dependence of the normalized fitted populations in the different states. The OD$\cdots$Cl$^-$ contribution shows a much slower vibrational relaxation.
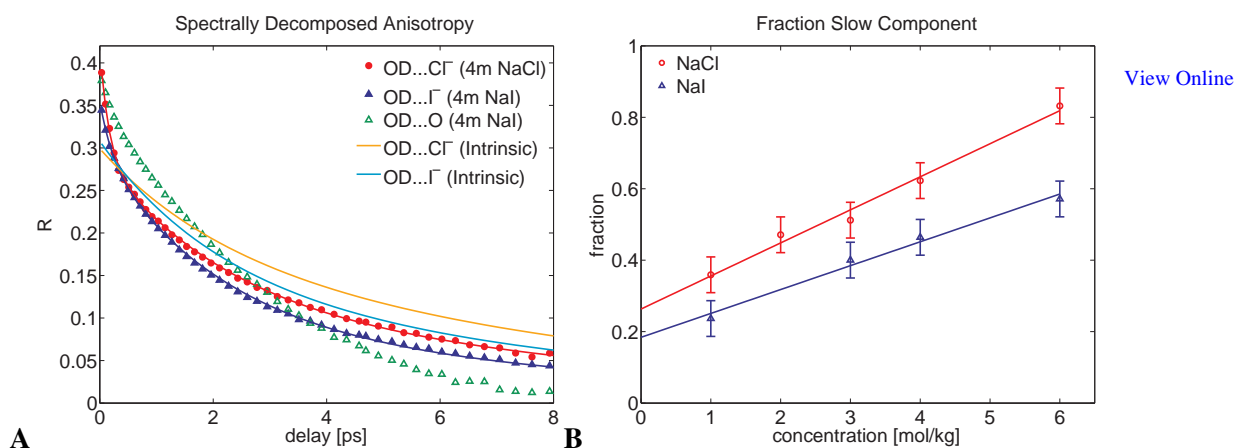
FIG. 5: (**A**) The anisotropy dynamics of the OD$\cdots$A$^-$ and OD$\cdots$O components. The intrinsic anisotropy decays are obtained by fitting equation 5 to the data. In the fits the exchange effects are included. The solid lines through the data points represent the fits including the initial drop due to librational motions. (**B**) The amplitude of the slow component of the intrinsic OD$\cdots$A$^-$ anisotropy curves at different concentrations.
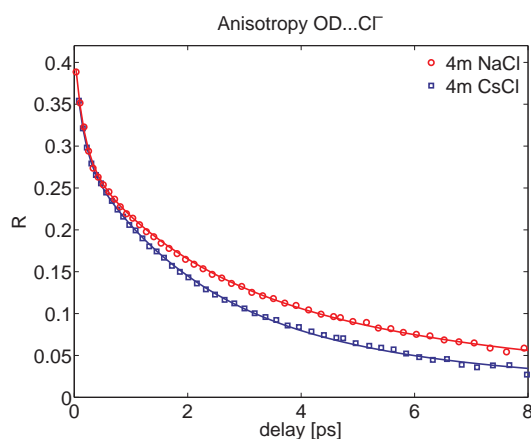
FIG. 6: The anisotropy decay of OD groups bound to chloride depends on the nature of the cation. The stronger hydrated Na$^+$ induces a smaller amplitude for the wobbling component than the weakly hydrated Cs$^+$.
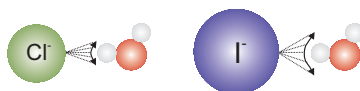
FIG. 7: The hydrogen bond between a water molecule and an anion has the freedom to wobble. For larger anions, the angular spread of the wobbling is larger.

25
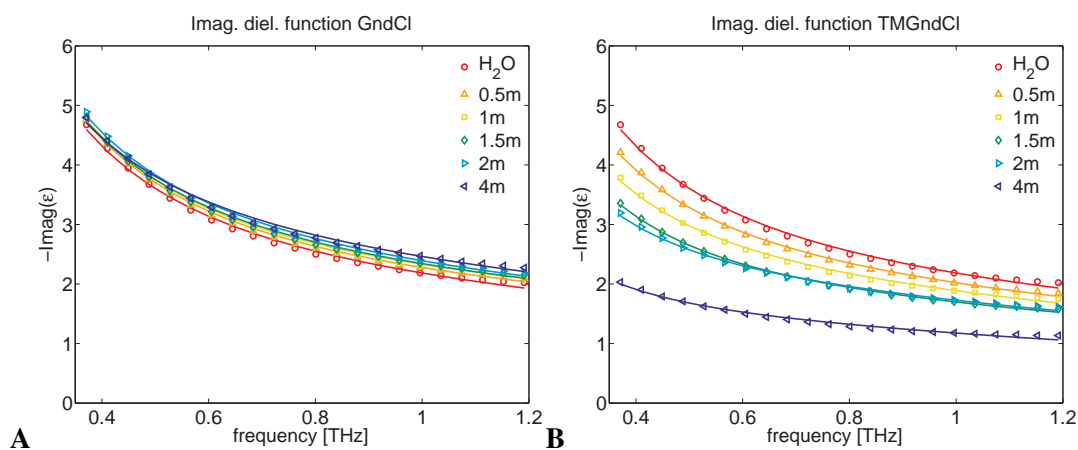
FIG. 8: The imaginary part of the dielectric function of (**A**) GndCl and (**B**) TMGndCl solutions of different concentrations.
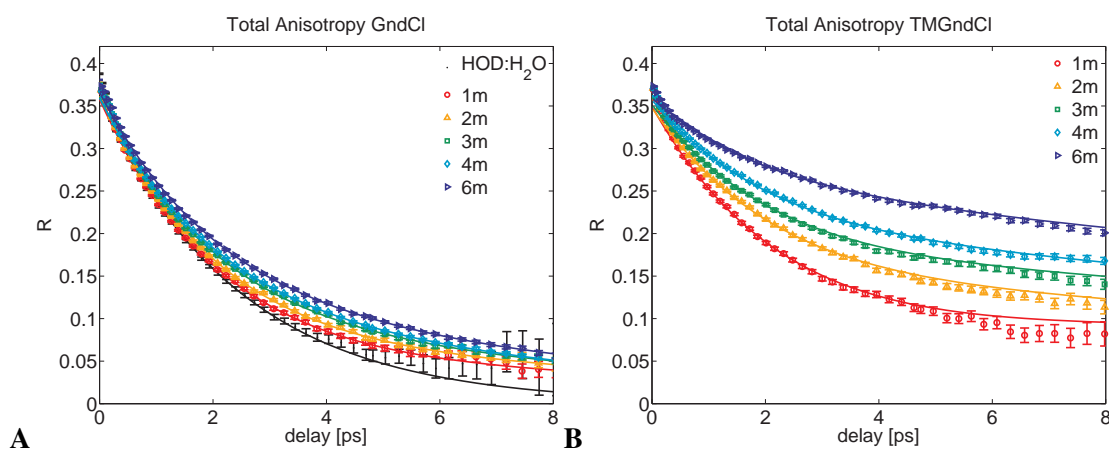

FIG. 9: The total anisotropy decay for solutions containing different concentrations of GndCl and TMGndCl. The substitution of hydrogen atoms by methyl group has a dramatic slowing down effect on the anisotropy decay.
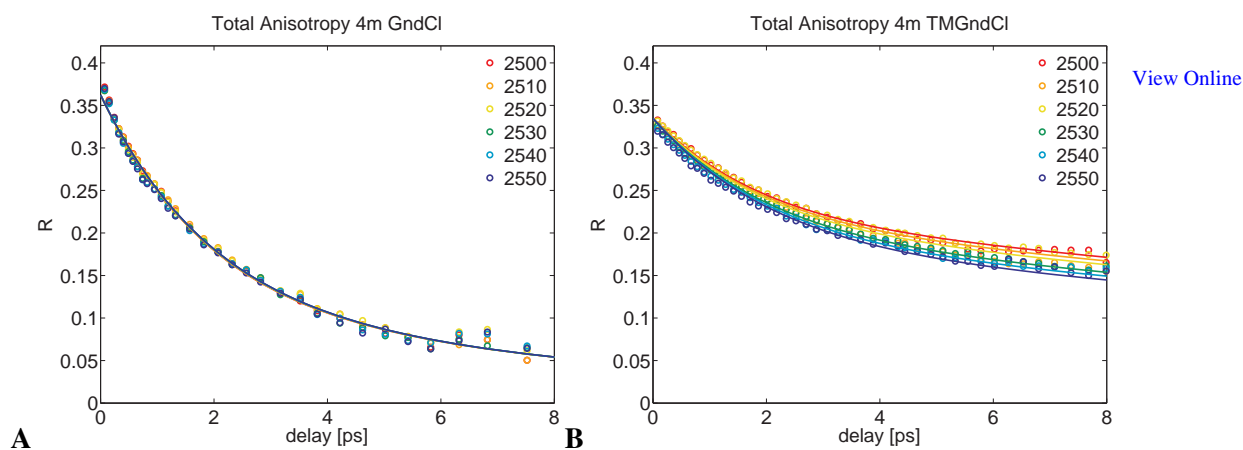
FIG. 10: Anisotropy decay curves for solutions of GndCl (**A**) and TMGndCl (**B**). The solutions of TMGndCl show a frequency dependence in their total anisotropy which is absent for solutions of GndCl. This frequency dependence shows that spectral diffusion in the TMGndCl solutions is very slow.
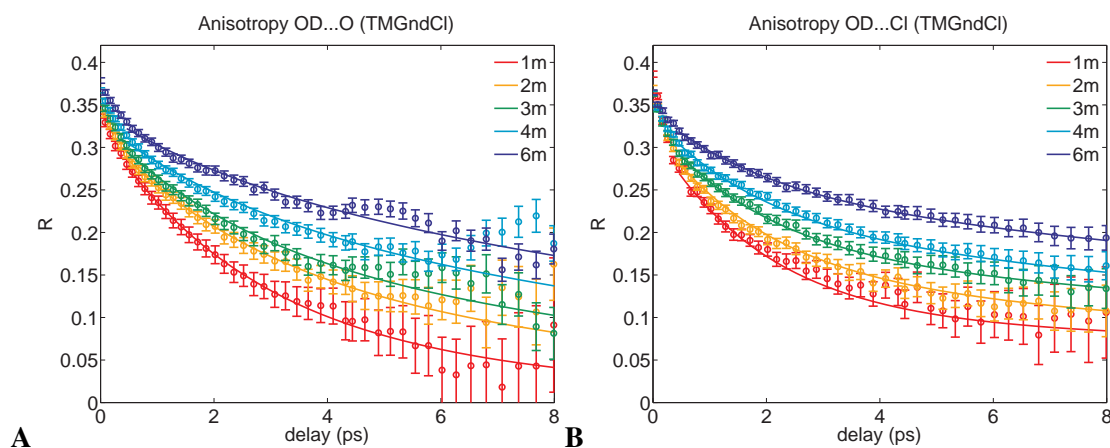

FIG. 11: Anisotropy decays of OD$\cdots$O (**A**) and OD$\cdots$Cl$^-$ (**B**) for different concentrations of TMGndCl. The hydrophobic groups of the cation slow down the dynamics of the water hydrogen-bond network outside the anion hydration shell, and thereby also decelerate the wobbling motion of the chloride bound OD groups.
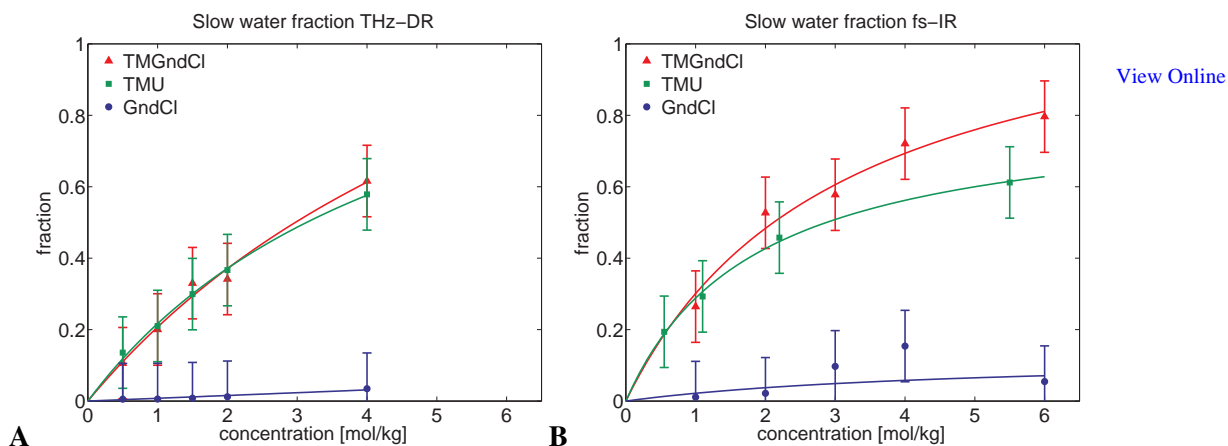
FIG. 12: (**A**) Slow water fractions obtained from the THz-DR measurements. For both experiments hardly any effect is seen for GndCl, while the effects for TMGndCl and TMU are almost identical. The slow water fractions for GndCl and TMU were calculated with data from [13] and [19] respectively. (**B**) Slow water fractions of the OD$\cdots$O anisotropy decays obtained from the fs-IR measurements. The data for TMU are taken from ref. [64].
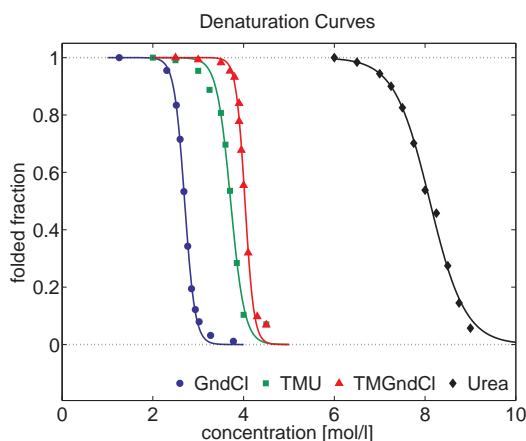

FIG. 13: Fraction of folded protein PYP as a function of denaturant concentration for different denaturants. The measurements were performed for a buffered solution at pH 7.